Bioresource Technology 146 (2013) 89–100

Contents lists available at SciVerse ScienceDirect

Bioresource Technology

journal homepage: www.elsevier.com/locate/biortech

A model for customising biomass composition in continuous microalgae production

Anne J. Klok [a,b,*], Johannes A. Verbaanderd [a], Packo P. Lamers [a], Dirk E. Martens [a], Arjen Rinzema [a], René H. Wijffels [a]

[a] Bioprocess Engineering, AlgaePARC, Wageningen University, PO Box 8129, 6700 EV Wageningen, The Netherlands
[b] Wetsus - Center of Excellence for Sustainable Water Technology, PO Box 1113, 8900 CC Leeuwarden, The Netherlands

HIGHLIGHTS

- Algal biomass composition was modelled as a function of nitrogen and light supply.
- The model is based on the electron distribution in *Neochloris oleoabundans*.
- Starch is the primary storage component; its production is linked to growth.
- 8.6% of excess electrons caused by N limitation ends up in storage lipids (TAG).
- Starch, TAG and protein require very different optimal cultivation conditions.

GRAPHICAL ABSTRACT

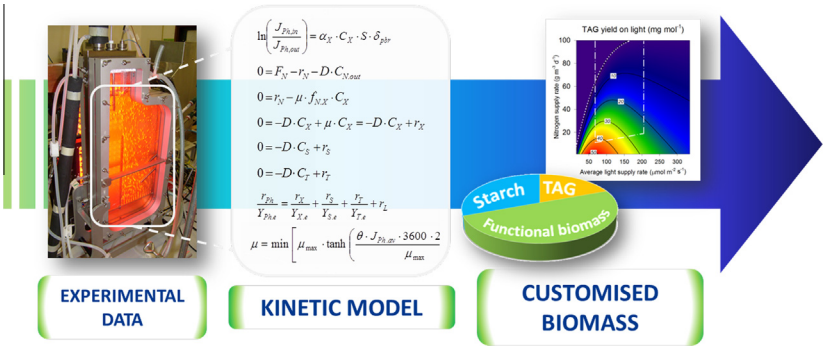

ARTICLE INFO

Article history:
Received 29 May 2013
Received in revised form 6 July 2013
Accepted 11 July 2013
Available online 18 July 2013

Keywords:
Microalgae
Biomass composition
Kinetic model
Storage lipids
Starch

ABSTRACT

A kinetic model is presented that describes functional biomass, starch and storage lipid (TAG) synthesis in the microalga *Neochloris oleoabundans* as a function of nitrogen and light supply rates to a nitrogen-limited turbidostat cultivation system. The model is based on the measured electron distribution in *N. oleoabundans*, which showed that starch is the primary storage component, whereas TAG was only produced after an excess of electrons was generated, when growth was limited by nitrogen supply. A fixed 8.6% of the excess electrons ended up in TAG, suggesting close metabolic interactions between nitrogen assimilation and TAG accumulation, such as a shared electron pool. The proposed model shows that by manipulating the cultivation conditions in a light or nitrogen limited turbidostat, algal biomass composition can be customised and the volumetric productivities and yields of the major biomass constituents can be changed on demand.

1. Introduction

Microalgae are considered promising candidates for the sustainable production of numerous products. These products range from pigments, poly-unsaturated fatty acids and proteins for the food or pharmaceutical market, to storage compounds such as triacylglyceride (TAG) or starch as raw materials for biofuel and commodity materials (Mata et al., 2010). However, when aiming at competitive production of microalgal products for the commodity market, the full potential of algal biomass must be exploited to compensate for the current production cost (Harrison et al., 2013; Wijffels et al., 2010). This biorefinery concept implies that total biomass composition will largely determine the profit that can be made on an algal product.

As the composition of algal biomass is heavily dependent on the culture conditions, manipulating these conditions can be a strategy

* Corresponding author Tel.: +31 (0) 317 485 012.
E-mail address: anne.klok@wur.nl (A.J. Klok).
URL: http://www.wageningenur.nl/bpe (A.J. Klok).

0960-8524/$ - see front matter © 2013 Elsevier Ltd. All rights reserved.
http://dx.doi.org/10.1016/j.biortech.2013.07.039

Nomenclature

α_X	absorption cross section of dry functional biomass in red light ($m^2\ g^{-1}$)
$\alpha_{X.min}$	hypothetical minimum absorption cross section of dry functional biomass in red light ($m^2\ g^{-1}$)
C_i	concentration of compound i ($g\ m^{-3}$)
D	dilution rate (d^{-1})
δ_{pbr}	light path of the photobioreactor (m)
f_i	mass fraction of compound i in dry biomass (g (g DW)$^{-1}$)
F_N	volumetric nitrogen supply rate ($g\ N\ m^{-3}\ d^{-1}$)
$f_{N.X}$	mass fraction of nitrogen in dry functional biomass (g (g DW)$^{-1}$)
HL	high light conditions
$J_{Ph.av}$	average photon flux density experienced by the algae ($\mu mol\ m^{-2}\ s^{-1}$)
$J_{Ph.in}$	photon flux density entering the system ($\mu mol\ m^{-2}\ s^{-1}$)
$J_{Ph.out}$	photon flux density leaving the system ($\mu mol\ m^{-2}\ s^{-1}$)
k_D	specific cell decay rate (d^{-1})
LL	low light conditions
μ	specific growth rate (d^{-1})
μ_{ref}	specific growth rate under light limited reference conditions (d^{-1})
r_i	volumetric production rate of compound i ($g\ m^{-3}\ d^{-1}$)
r_L	rate of electrons lost in catabolism or dissipation processes ($mol\ e^-\ m^{-3}\ d^{-1}$)
r_N	volumetric nitrogen consumption rate ($g\ N\ m^{-3}\ d^{-1}$)
$r_{N.ref}$	volumetric nitrogen consumption rate under light limited reference conditions ($g\ N\ m^{-3}\ d^{-1}$)
r_{Ph}	volumetric photon absorption rate ($mol\ \gamma\ m^{-3}\ d^{-1}$)
σ	slope, as determined by linear regression
S	starch
S	scattering correction coefficient (−)
θ	initial slope that relates irradiance to growth rate in the hyperbolic tangent model for algal growth ($m^2\ mol^{-1}$)
T	TAG (Triacylglyceride)
X	functional biomass (i.e. non starch or TAG)
$Y_{i.e}$	yield of compound i on electrons (g (mol e$^-$)$^{-1}$)
$Y_{Ph.e}$	minimum theoretical quantum requirement for electron release from water (mol γ (mol e$^-$)$^{-1}$)

for obtaining a tailor-made biomass composition (Harrison et al., 1990). For example, nitrogen depletion is the preferred strategy to increase TAG and starch fractions in biomass, at the expense of protein synthesis which requires the presence of nitrogen in the growth medium (Ball et al., 1990; Hu et al., 2008). Nitrogen availability directly influences the balance between energy absorbed in the photosystems and reducing potential used in anabolism, as up to 55% of microalgal carbon assimilation is coupled to nitrogen assimilation (Huppe and Turpin, 1994). Based on this close interaction, it is often hypothesised that under nitrogen limitation, the excess of reducing potential and energy produced in the photosystems can be used in the synthesis of storage compounds (Li et al., 2013). This helps to maintain a safe level of reducing potential in the photosystems and thus to prevent damage to the photosystems (Ledford and Niyogi, 2005), while at the same time energy is stored (Hu et al., 2008; Li et al., 2010).

Besides resulting in storage compound accumulation, nitrogen limitation has as an undesirable effect: more energy is dissipated in the photosystems in order to equilibrate the energy imbalance (Kolber et al., 1988) and this strongly reduces the carbon assimilation capacity of the alga (Turpin, 1991). Recently we have shown that energy dissipation is the predominant mechanism for dealing with an excess of reducing potential in the photosystems in *Neochloris oleoabundans* cultivated under nitrogen limitation (Klok et al., 2013). This links storage compound accumulation to a lower yield of algal biomass on available light, which is detrimental for production economics, as yield on light is directly proportional to the aerial productivity (Richmond, 2004).

Understanding the interactions between nitrogen assimilation, storage compound accumulation and photosynthesis will help to determine the optimal culture conditions for obtaining biomass of a desired composition. Several models have been developed that describe the effects of light and nutrient supply on photosynthesis, growth, TAG and/or carbohydrate accumulation in microalgae in batch (Packer et al., 2011; Quinn et al., 2011) and continuous processes (Mairet et al., 2011). However, to date no model is available that evaluates biomass composition, as well as the productivities and yields of separate biomass components as a function of cultivation conditions and as such explores the potential of algal biomass as a whole.

In this paper a kinetic model is presented that describes the combined effect of nitrogen and light supply on the electron distribution in microalgal cells, and on the biomass composition that is the result of this electron distribution. Based on the electron distribution, productivities and yields on light could be calculated for the major biomass components; functional biomass (rich in protein), starch and TAG. Previously obtained data of *N. oleoabundans* grown under both nitrogen and light limitation in a flat panel photobioreactor, operated as a turbidostat, was used to derive the model equations and parameters (Klok et al., 2013). Turbidostat control in a photobioreactor allows for steady state conditions in which the light absorption of the culture is fixed. Combining this type of control with a separate continuous nitrogen supply allows for controlling the ratio between nitrogen uptake rate and energy intake in steady state cultures. These stable conditions enable thorough investigation of the effect of the imposed stress on cell physiology, without the complicating effects of changing environmental conditions that are typically observed in batch experiments.

The model shows that reducing the electron flux towards functional biomass by limiting the nitrogen supply rate, gives control over the electron distribution in *N. oleoabundans*. As a result, the macromolecular composition of biomass can be steered into many directions.

2. Methods

2.1. Photobioreactor set-up and experimental conditions

N. oleoabundans was grown in a turbidostat operated flat panel photobioreactor, with a nitrogen feed separate from the diluting medium (Klok et al., 2013). This type of system allows for independent control of the light absorption and nitrogen supply rates of the culture. In this way, combinations of excess light absorption and growth-limiting nitrogen supply rates can be applied, which results in accumulation of storage compounds such as TAG, while at the same time maintaining a dividing algal population. Because growth and storage accumulation are taking place simultaneously under steady state conditions, the system is well suited to study the interactions between growth, nitrogen assimilation and

storage metabolite accumulation. This as opposed to the use of classic nitrogen starvation (i.e. batch) experiments for the evaluation of growth and nitrogen stress in microalgae, where growth and storage metabolite accumulation are taking place in different experimental phases.

In a nitrogen limited turbidostat, F_N (the nitrogen supply rate, in g m^{-3} d^{-1}), $J_{Ph.in}$ (photon flux density entering the system, in μmol m^{-2} s^{-1}) and $J_{Ph.out}$ (photon flux density leaving the system, in μmol m^{-2} s^{-1}) were the only control variables, and therefore these variables are used as the only input for the model presented in this paper. Algae were grown under two light regimes: average photon absorption rates (r_{Ph}) of 762 ± 4 (low light conditions) and 1684 ± 4 mol m^{-3} d^{-1} (high light conditions) resulted from a $J_{Ph.in}$ of 193 and 460 μmol m^{-2} s^{-1} and a $J_{Ph.out}$ of 17 ± 1 and 70 ± 1 μmol m^{-2} s^{-1}, for low and high light conditions respectively. These light regimes were combined with several nitrogen supply rates to the system and resulted in 9 steady states, for which growth rate, medium composition, biomass concentration and biomass composition (TAG, starch, nitrogen content, ash content and absorptive cross section) were measured. For more details on this experiment and the analyses see (Klok et al., 2013). Three additional analyses were carried out and are discussed below. A summary of all relevant measurements can be found in Appendix A.

2.2. Additional measurements

Biomass samples were collected on ice over a period of exactly 24 h in each steady state. Starch was measured in the lyophilized biomass samples using a commercial kit (Total Starch (AA/AMG), Megazyme International, Bray, Ireland).

The supernatant of the 24 h samples was evaluated for TOC (Total Organic Carbon), which was measured as the difference between total carbon (TC) and inorganic carbon (IC), using a TOC–V_{CPH}/TOC–V_{CPN} Total Organic Carbon Analyser (Shimadzu corp, Kyoto, Japan). With the determination of dissolved organic carbon, the measured biomass concentrations ($C_{measured}$ in g DW m^{-3}) were corrected for any biomass lost due to cell lysis (C_{TOC} in g DW m^{-3}), assuming that all organic material in solution had the same elemental composition as suspended biomass. The corrected biomass concentrations (C_{TOTAL} in g DW m^{-3}) were then used as input for the model.

The dark respiration rate was determined using a biological oxygen monitor (BOM) (Hansatech Instruments Limited, Norfolk, England), as described by (Sousa et al., 2012).

3. Theory

3.1. Electron distributions

Fig. 1A presents a schematic overview of the distribution of photon-derived electrons over the algal cell. Light energy (r_{Ph}) is used to drive electrons from water into the electron transport chain. At the end of the chain, electrons are donated to temporary electron carriers, such as NADPH, and algae use the reducing power stored in these carriers to fix carbon and construct the molecules that make up the algal cell (total biomass). Electrons either end up in functional biomass (r_X), which is rich in proteins, or in the storage products starch (r_S) and TAG (r_T), which are accumulated in starch granules and lipid bodies, respectively. Not all light energy that is absorbed by an alga is used to liberate electrons that end up in new cell material. Part of the light energy is dissipated in the photosystems and in addition part of the electrons ending up in NADPH is returned to oxygen, forming water and generating ATP for catabolism. In this paper the term 'catabolism' is used for the collection of all processes that use respiratory ATP for the synthesis and assembly of biomass constituents including the storage polymers, or energy that is necessary for cellular maintenance (Kliphuis et al., 2012). 'Dissipation' refers to the processes of chlorophyll fluorescence and heat production in the chloroplast (Kolber et al., 1988; Pan et al., 2011), which are used to adjust electron production rates to the actual demand for electrons in lower metabolism. Both catabolism and dissipation are considered as a loss of electrons in this model, because these processes do not result in the incorporation of electrons into the molecules that make up cell material. Both processes are therefore represented in the remaining, rate of electron loss (r_L).

3.2. Assumptions

The following assumptions were made for the model:

- No other electrons sinks are produced besides functional biomass, starch and TAG.
- The first priority of an alga is to use the available electrons for its maintenance requirements, the second priority is to produce functional biomass (Meeuwse et al., 2011).
- Functional biomass production is either limited by the supply of light or by the supply of nitrogen source. All other necessary nutrients are present in abundance.
- Nitrate uptake rates are independent of external nitrate concentrations (zero order kinetics).

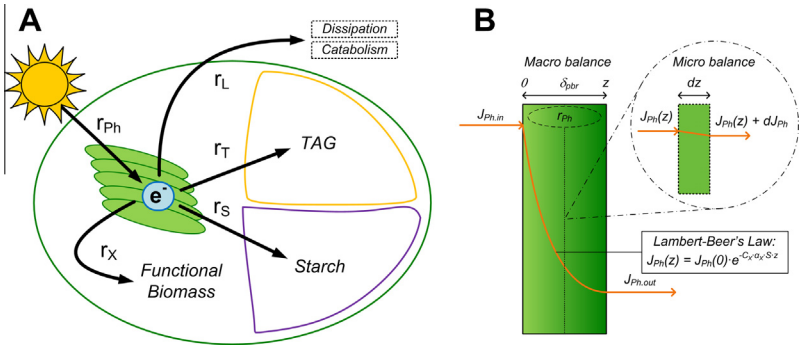

Fig. 1. (A) Schematic representation of the electrons distribution over the microalgal cell. Photons (r_{Ph}) are absorbed and used to drive electrons from water. These end up in functional biomass (r_X), TAG (r_T) and starch (r_S). r_L represents the light energy that was dissipated in the thylakoids as well as the rate of photon-derived electrons that is used for the generation of ATP (catabolism), and as such does not end up in cell material. (B) Schematic representation of light distribution in the culture vessel. A macro balance was constructed to obtain the volumetric photon absorption rate (r_{Ph}) of the whole culture (Eq. (1)). A micro balance was constructed to describe the light profile inside the culture (Eq. (2)). Integration of this micro balance gives Lambert–Beer's law (Eq. (3)).

- Starch is the primary storage component during growth and therefore its production rate is proportional to functional biomass production.
- TAG is only produced under nitrogen limitation.
- There is no maximum to the TAG or starch fraction in an algal cell, and no minimum to the fraction of functional biomass for sustaining cell division.
- The composition of TAG is constant, and equal to the average composition of TAG measured in the turbidostat experiments.
- TAG and starch do not absorb light. They can, however, cause scattering of the light.
- When moving through the light gradient in the reactor, algae adapt to the average light intensity that they experience, and the specific growth rate under light limiting conditions is the result of this average experienced light intensity.
- A minimum quantum requirement ($Y_{Ph.e}$) of 2 photons per electron was assumed for the light-driven liberation of electrons from water, which is in agreement with the Z-scheme of photosynthesis.
- Absorption of photons always results in the generation of electrons. Energy dissipation processes and photosynthetic inefficiencies are therefore accounted for in the model as electron losses.

3.3. Balances

The model is based on balances for absorbed light and consumed nitrogen, the products that are formed (X, T and S) in the system, and for the electrons that are the intermediate between substrates and products. These balances are discussed in the following sections; a summary can be found in Table 1.

3.3.1. Light

A macro balance can be derived for the volumetric photon absorption rate over the system (Fig. 1B):

$$0 = (J_{Ph.in} - J_{Ph.out}) \cdot 3600 \cdot 24 \cdot 10^{-6} - r_{Ph} \cdot \delta_{pbr} \quad (1)$$

with r_{Ph} as the rate of photons absorbed by the algae in mol photons m^{-3} d^{-1}, δ_{pbr} as the culture depth (m) and $J_{Ph.in}$ and $J_{Ph.out}$ (μmol m^{-2} s^{-1}) as the photon fluxes entering and leaving the culture, respectively. Secondly, a micro balance can be derived for an arbitrary, infinitively small slice (dz) parallel to the illuminated side of the culture vessel (Fig. 1B):

$$0 = -dJ_{Ph} - \alpha_X \cdot C_X \cdot J_{ph} \cdot S \cdot dz \quad (2)$$

with dJ_{Ph} as the change in photon flux (mol m^{-2} s^{-1}) over dz (m), which is caused by the absorption of light by functional biomass (C_X in g m^{-3}) with a certain absorption cross section of dry functional biomass (α_X in m^2 g^{-1}). Integration of the micro balance gives Lambert–Beer's law, a function that describes transmission in a solution as a function of concentration, absorption characteristics and length of the light path. Lambert–Beer's law only describes absorptive effects and does not account for light scattering in algal suspensions. Scattering largely depends on the concentration of biomass in the system (Yun and Park, 2001). It effectively causes a lengthening of the light path, increasing the probability of absorp-

Table 1
Balances over the system with their target variables (i.e. the variables that are calculated from the balances) and other unknowns.

#	Component	Balance	Target variable	Other unknowns
[1]	Light macro	$0 = (J_{Ph.in} - J_{Ph.out}) \cdot 3600 \cdot 24 \cdot 10^{-6} - r_{Ph} \cdot \delta_{pbr}$	$\boldsymbol{r_{Ph}}$	–
[3]	Light micro	$\ln\left(\frac{J_{Ph.in}}{J_{Ph.out}}\right) = \alpha_X \cdot C_X \cdot S \cdot \delta_{pbr}$	$\boldsymbol{C_X}$	α_X, S
[4]	Nitrate	$0 = F_N - r_N - D \cdot C_{N.out}$	$\boldsymbol{r_N}$	D, $C_{N.out}$
[5]	Nitrogen	$0 = r_N - \mu \cdot f_{N.X} \cdot C_X$	$\boldsymbol{\mu}$	r_N, $f_{N.X}$, C_X
[6]	Biomass	$0 = -D \cdot C_X + \mu \cdot C_X = -D \cdot C_X + r_X$	$\boldsymbol{r_X}$	D, C_X, μ
[7]	Starch	$0 = -D \cdot C_S + r_S$	$\boldsymbol{C_S}$	D, r_S
[8]	TAG	$0 = -D \cdot C_T + r_T$	$\boldsymbol{C_T}$	D, r_T
[9]	Electrons	$\frac{r_{Ph}}{Y_{Ph.e}} = \frac{r_X}{Y_{X.e}} + \frac{r_S}{Y_{S.e}} + \frac{r_T}{Y_{T.e}} + r_L$	$\boldsymbol{r_L}$	(r_X/$Y_{X.e}$), (r_S/$Y_{S.e}$) and ($Y_{T.e}$/ $Y_{T.e}$)

tion within the microalgal culture. A scattering factor S was used to correct for the scattering effect of cells (Section 4.1.7). Integration of dJ_{PH} over the entire culture depth (δ_{pbr}) results in:

$$\ln\left(\frac{J_{Ph.in}}{J_{Ph.out}}\right) = \alpha_X \cdot C_X \cdot S \cdot \delta_{pbr} \quad (3)$$

3.3.2. Nitrogen

Two balances are needed for nitrogen: a component balance for the nitrate that is supplied to the system, and a balance for the nitrogen atoms that are used by the algae:

$$0 = F_N - r_N - D \cdot C_{N.out} \quad (4)$$

$$0 = r_N - \mu \cdot f_{N.X} \cdot C_X \quad (5)$$

in which F_N represents the volumetric nitrate supply rate to the system (g N m^{-3} d^{-1}), r_N the volumetric nitrogen consumption rate (g N m^{-3} d^{-1}), D the dilution rate(d^{-1}), $C_{N.out}$ (g N m^{-3}) the concentration of nitrate in the outgoing medium, μ the specific growth (d^{-1}), $f_{N.X}$ the fraction of nitrogen in functional biomass (g N (g DW)$^{-1}$) and C_X the concentration of functional biomass in the system (g m^{-3}). In the experiments, two limitations were set by separately controlling the rates of nitrate supply and light absorption in the turbidostat. Either the nitrate supply was sufficient to sustain light limited growth and therefore $C_{N.out} > 0$, or the nitrate supply rate was insufficient for light limited growth and it was assumed that $C_{N.out} = 0$. In the latter situation, F_N is equal to r_N.

3.3.3. Products

The balances for functional biomass (X), starch (S) and TAG(T) read, respectively:

$$0 = -D \cdot C_X + \mu \cdot C_X = -D \cdot C_X + r_X \quad (6)$$

$$0 = -D \cdot C_S + r_S \quad (7)$$

$$0 = -D \cdot C_T + r_T \quad (8)$$

Eq. (6) shows that under steady state conditions the specific growth rate (μ) equals the dilution rate (D). Eqs. ())(6)–(8) can be used to find the concentrations of X, S and T in the system (C_X, C_S and C_T, respectively, in g m^{-3}) from the volumetric production rates (r_X, r_S and r_T, respectively, in g m^{-3} d^{-1}). The latter rates are derived from the electron distributions in the cell (Sections 4.1.1–4.1.3). When all concentrations are known, the biomass composition (i.e. the fractions of X, S and T) can be calculated.

3.3.4. Electrons

The electron balance is derived from the simplified distribution of electrons in the cell that is presented in Fig. 1A:

$$\frac{r_{Ph}}{Y_{Ph.e}} = \frac{r_X}{Y_{X.e}} + \frac{r_S}{Y_{S.e}} + \frac{r_T}{Y_{T.e}} + r_L \quad (9)$$

r_{Ph} represents the rate of light absorption in the system (mol photons m^{-3} d^{-1}) and r_X, r_S and r_T the production rates of X, S and T, respectively (g m^{-3} d^{-1}). $Y_{Ph.e}$ is the minimum theoretical quantum requirement for electron release from water, which is 2 mol photons per mol electrons generated. $Y_{X.e}$, $Y_{L.e}$ and $Y_{S.e}$ represent the yields of biomass, TAG and starch on electrons that end up in the product (g (mol e^-)$^{-1}$). These yields can be calculated from the degree of reduction of each product (Appendix B). r_L represents the rate of electrons that do not end up in cell constituents X, S or T (mol m^{-3} d^{-1}), either because electrons are used for ATP generation needed for maintenance and biomass formation (catabolism), or because part of r_{Ph} is dissipated before any electrons are liberated from water. For simplicity it was assumed that absorbed photons are always used to generate electrons and that these electrons are subsequently dissipated. Therefore $r_{Ph}/Y_{Ph.e}$ is referred to as the rate of electron generation throughout this paper. This implies that diversion from the minimum quantum requirement due to photosynthetic inefficiency is accounted for in r_L.

4. Results and discussion

4.1. Additional equations

All variables in the balances (Table 1) are a function of the rates of light absorption (r_{Ph}) and volumetric nitrogen supply rate (F_N), which can be controlled independently in the nitrogen limited turbidostat. Additional equations are needed to calculate the production rates and fractions of functional biomass, TAG and starch under nitrogen limitation. These were derived based on the measured electron distributions and some additional experimental results (growth rate, absorptive cross section and scattering), as a function of nitrogen and light supply rates. A summary of the relevant experimental data can be found in Appendix A, the calculations of the rates at which electrons are incorporated into the three biomass constituents in Appendix B. It should be noted that it was assumed that the small TAG fraction (f_{TAG}) observed in the reference conditions (light limited growth; [A] and [E]), as reported in Klok et al., (2013), is a part of functional biomass, and therefore all values of f_{TAG} were corrected for the value measured in the reference condition.

4.1.1. Functional biomass

As the nitrogen supply rate was progressively reduced, the fraction of electrons incorporated in functional biomass decreased (Fig. 2). All assimilated nitrogen ends up in functional biomass (X), the rate of electrons ending up in X ($r_X/Y_{X.e}$) was assumed to be proportional to the nitrogen assimilation rate r_N (Fig. 3A). A linear correlation ($R^2 = 0.99$) with a slope (σ_N) of 2.38 ± 0.04 mol e^- g^{-1} N assimilated was found when the intercept was forced to zero:

$$\frac{r_X}{Y_{X.e}} = \sigma_N \cdot r_N \quad (10)$$

This shows that the electrons ending up in functional biomass that contains one gram of nitrogen (σ_N) was constant over the range of experiments, regardless of the light intensity used, regardless whether nitrogen supply was sufficient or limiting, and regardless of changes in the nitrogen content of functional biomass ($f_{N.X}$; see

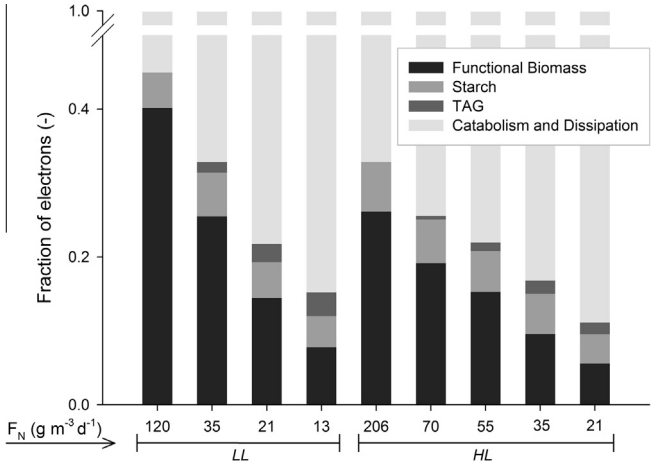

Fig. 2. Electron distributions for the nitrogen limitation experiment at several nitrogen supply rates and two different light regimes; low (LL) and high light conditions (HL).

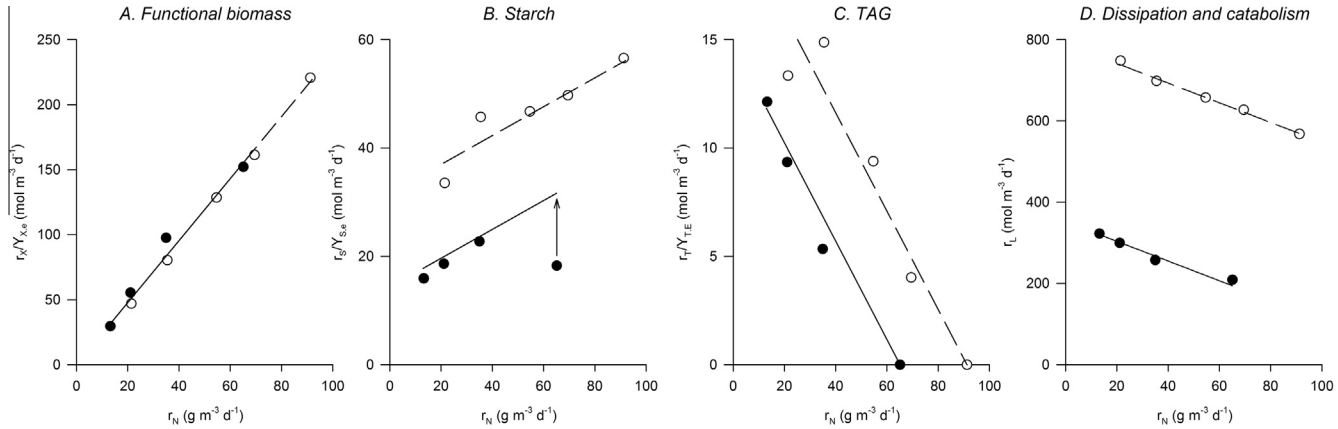

Fig. 3. The electrons ending up in functional biomass (A), electrons ending up in starch (B), electrons ending up in TAG (C) and electrons lost in dissipation and catabolic processes (D) as function of r_N. Closed circles represent experiments that were performed under low light conditions, open circles represent experiments performed under high light conditions. Lines represent the fit of the model equations to the data, within the experimental range.

Appendix A). Eq. (10) allows calculation of $r_X/Y_{X.e}$ for any combination of light absorption and nitrogen uptake rates. It should be noted, however, that $Y_{X.e}$ (the yield X on electrons, in g (mol e$^-$)$^{-1}$) was not a constant, and that r_X did not decrease proportionally with r_N. Consequently, r_X could not be calculated using Eq. (10). Therefore, additional equations were derived (Sections 4.1.5–4.1.7), that allowed for calculation of μ and C_X as a function of light and nitrogen supply rates. Subsequently, the balance for functional biomass (Eq. (6)) was used to obtain r_X.

4.1.2. Starch

The rate of electrons ending up in starch decreased as nitrogen assimilation declined (Fig. 2), indicating that starch does not have a secondary, nitrogen stress related storage function, but a storage

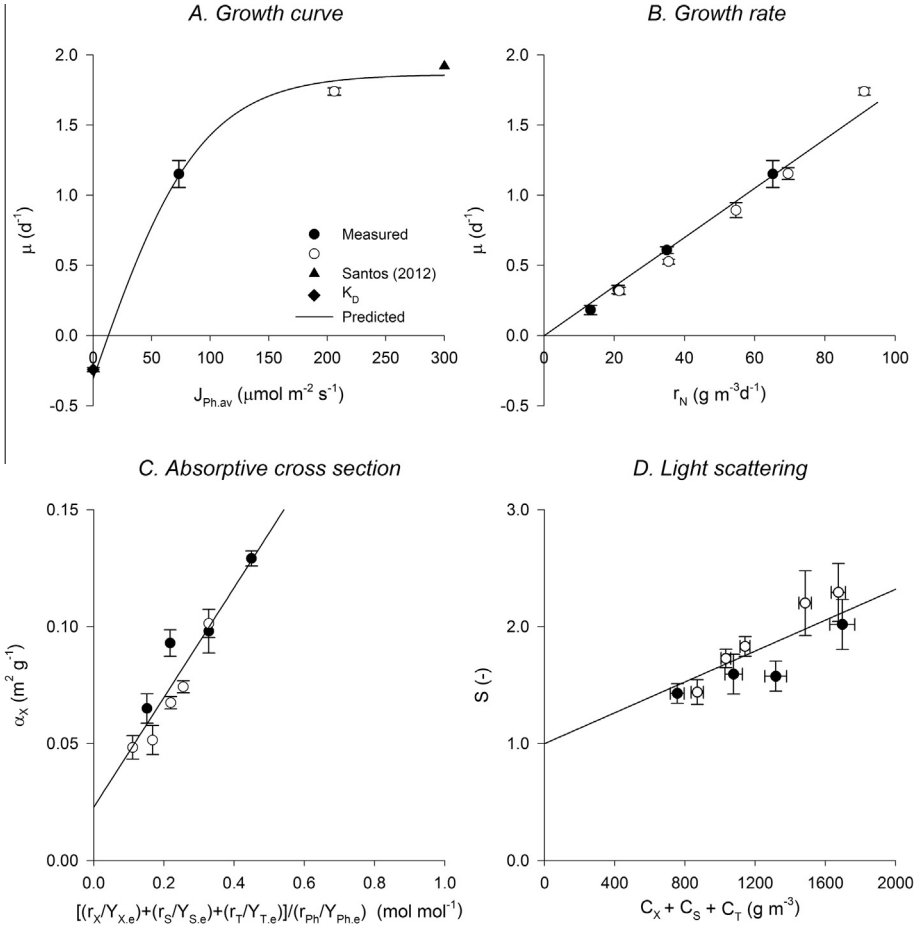

Fig. 4. Fitted growth curve of *Neochloris oleoabundans* (A); specific growth rate (μ) and nitrogen consumption rate (r_N) are proportional (B); absorptive cross section (α_X) is proportional to the ratio between electrons ending up in biomass constituents X, T and S and the electrons that could be generated from the absorbed light (C); light scattering is proportional to $C_X + C_S + C_T$ (D): closed circles represent experiments that were performed under low light conditions, open circles represent experiments performed under high light conditions. Lines represent the fit to the mentioned equations.

function related to growth. This is in agreement with findings of Li et al., (2011), who found a decreased starch content in *Pseudochlorococcum* sp. after prolonged nitrogen depletion, combined with a decrease in activity of ADP-glucose pyrophosphorylase (AGPase), the enzyme that catalyses the first committed step of starch synthesis. Moreover, Rismani-Yazdi et al. (2012) observed a reduction of AGPase and starch synthase, which catalyses the subsequent step in starch synthesis, in *N. oleoabundans* grown under nitrogen depleted conditions. (Cohen and Parnas, 1976; Turpin, 1991) also suggested that starch synthesis has a growth related function: starch is used to store energy during the day, which can be employed to power several processes in the absence of light, such as cell division, the assimilation of nitrogen and maintenance.

The number of electrons ending up in starch was proportional to the number of electrons ending up in functional biomass (or to r_N, according to Eq. (10)), with an intercept dependent on the light supply rate (Fig. 3B):

$$\frac{r_S}{Y_{S.e}} = \sigma_S \cdot \frac{r_X}{Y_{X.e}} + \sigma_M \cdot \frac{r_{Ph}}{Y_{Ph.e}} = \sigma_S \cdot \sigma_N \cdot r_N + \sigma_M \cdot \frac{r_{Ph}}{Y_{Ph.e}} \quad (11)$$

This intercept indicates that a certain amount of starch is always produced, even when there is no functional biomass production. Such production might be related to storage of starch for maintenance purposes. Furthermore, the damaging effect of increased light supply rates might explain why algae store more starch at higher light intensities, as photosystem repair rates increase under elevated light supply rates (Melis, 1999).

The measured starch production rate at $r_x/Y_{X.E}$ = 152 mol m^{-3} d^{-1} and low light conditions ([A] in Fig. 2) is an outlier to the observed trend in Fig. 3B, and was therefore not used to fit Eq. (11)1 to the data. The fit to the remaining 8 points gave σ_S = 0.112 - mol mol^{-1} and σ_M = 0.038 mol mol^{-1} (R^2 = 0.96). An explanation for the apparent outlier is that insufficient electrons were left for starch synthesis under this low average light intensity, because processes with a higher priority level, i.e. functional biomass production and catabolism, used most of the electrons generated. As catabolism cannot be distinguished from other electron losses in the model, it is accounted for in Eq. (11), and the model will therefore slightly overestimate the electrons used in starch synthesis at light limited growth conditions with low light supply rates.

4.1.3. TAG

As the amount of electrons ending up in TAG increased when less electrons were ending up in functional biomass and starch (Fig. 2), it was hypothesised that the rate at which electrons are channelled into TAG ($r_T/Y_{T.e}$) is proportional to the electron excess that is the result of a decrease in functional biomass and starch production compared to the light limited reference conditions:

$$\frac{r_T}{Y_{T.e}} = \sigma_T \cdot \left[\left(\frac{r_X}{Y_{X.e}} + \frac{r_S}{Y_{S.e}} \right)_{ref} - \left(\frac{r_X}{Y_{X.e}} + \frac{r_S}{Y_{S.e}} \right) \right] \quad (12)$$

The term between brackets represents the excess electrons not ending up in functional biomass and starch compared to the light limited reference situation and σ_T the fraction of these electrons (mol mol^{-1}) that is ending up in TAG. Eq. (12) can be combined with Eqs. (10) and (11), resulting in a function that is only dependent on light and nitrogen supply rates:

$$\frac{r_T}{Y_{T.e}} = \sigma_T \cdot \sigma_N \cdot (1 + \sigma_S) \cdot (r_{N.ref} - r_N) \quad (13)$$

in which $r_{N.ref}$ is the nitrogen consumption rate under light limitation (see Section 4.1.5). $r_T/Y_{T.e}$ was calculated for each steady state and linear regression to ($r_{N.ref} - r_N$) with intercept zero gave σ_T = 0.086 ± 0.005 mol mol^{-1} (R^2 = 0.97, see Fig. 3C, where $r_T/Y_{T.e}$ is plotted against r_N). This means, that in *N. oleoabundans*, 8.6% of the excess electrons resulting from nitrogen shortage, is used for TAG accumulation. A fixed percentage of 'excess' electron used for TAG synthesis suggests a close metabolic relationship between nitrogen assimilation and TAG accumulation. As nitrogen assimilation and the synthesis of fatty acids are mainly taking place in the plastid (Huppe and Turpin, 1994; Liu and Benning, 2013), both processes are drawing electrons from the same pool of reducing equivalents. This might explain why TAG synthesis can directly take up part of the excess electrons that are formed when nitrogen assimilation is limited, but it does not explain why this is such a small and constant part. Further studies of the sensing and regulating mechanisms involved in the energy distribution towards dissipation, maintenance, starch and TAG under nitrogen starvation are necessary to explain the fixed 8.6% that was found.

4.1.4. Energy loss

Electrons that do not end up in cell constituents are either used for generation of ATP for biomass synthesis or maintenance (catabolism), or lost in dissipation processes in the chloroplast. As it is difficult to distinguish these processes, they are lumped into one 'loss' term, which can be calculated by combining the electron balance (Eq. (9)), with Eqs. (10), (11), and (13):

$$r_L = \sigma_N \cdot (\sigma_T - 1) \cdot (\sigma_S + 1) \cdot r_N + (1 - \sigma_M) \cdot \frac{r_{Ph}}{Y_{Ph.e}} - \sigma_T \cdot \sigma_N \cdot (\sigma_S + 1) \cdot r_{N.ref} \quad (14)$$

In Fig. 3D it can be seen that the electron loss is indeed linearly dependent on the nitrogen consumption rate (r_N) (R^2 = 0.99). As, due to the decline in specific growth rate, ATP use for biomass synthesis is likely to decrease under nitrogen limitation, it is likely that dissipation processes are accounting for the bulk of the electron loss under nitrogen limitation, making dissipation a more important sink for excess reducing potential than TAG synthesis.

To calculate the production rates of X, S, and T from the electron distributions in the cell, the rate of electrons ending up in each component should be multiplied by the yield of that component on electrons. r_S and r_T could be calculated using Eqs. (11) and (12) as $Y_{S.e}$ and $Y_{T.e}$ are constants (for calculation, see Appendix B.II). However, $Y_{X.e}$ is not constant (Section 4.1.1) and therefore additional equations are derived in the following sections, that allow calculation of μ and C_X as a function of light and nitrogen supply rates. Subsequently, the balance for functional biomass (Eq. (6)) was used to obtain r_X. With μ (and thus D) known, the concentration of all biomass components and the biomass composition (i.e. f_X, f_S and f_T) can be calculated using Eqs. (6)–(8).

4.1.5. Specific growth rate

Growth is limited by either light supply or by nitrogen supply, the two input variables. In the first situation, residual nitrate is present in the outflow of the system and $F_N > r_N$. In the second situation, residual nitrogen is assumed to be zero and the nitrate balance (Eq. (4)) simplifies to $F_N = r_N$.

4.1.5.1. Light limitation: $F_N \geqslant r_N$. The hyperbolic tangent model (Platt and Jassby, 1976) was used to calculate the specific growth rate under light limited conditions (μ_{ref}). It was assumed that the specific growth rate under light limited growth conditions is a result of the average light intensity experienced by the cells. Therefore, the specific growth rate under light limited conditions is:

$$\mu_{ref} = \mu_{max} \cdot \tanh\left(\frac{\theta \cdot J_{Ph.av} \cdot 3600 \cdot 24 \cdot 10^{-6}}{\mu_{max}} \right) - k_D \quad (15)$$

with μ_{max} as the maximum specific growth rate (d^{-1}), and θ in m^2 mol^{-1}. k_D is the specific cell decay rate (d^{-1}), which is a measure for the minimal maintenance rate at $J_{Ph.av}$ = 0 μmol m^{-2} s^{-1}. $J_{Ph.av}$

($\mu mol\ m^{-2}\ d^{-1}$) in Eq. (15) can be calculated by dividing the integral of the light profile over the culture (Fig. 1B) by δ_{pbr}:

$$J_{Ph.av} = \frac{1}{\delta_{pbr}} \int_0^{\delta_{pbr}} J_{Ph}(z)dz = \frac{J_{Ph.in} - J_{Ph.out}}{\ln(J_{Ph.in}/J_{Ph.out})} \quad (16)$$

k_D was determined using *N. oleoabundans* adapted to the lowest tested $J_{Ph.av}$ (73 $\mu mol\ m^{-2}\ s^{-1}$). Cells were harvested from the reactor during steady state and a dark respiration rate of $11.3 \times 10^{-3} \pm 0.7 \times 10^{-3}$ mol O_2 $g^{-1}\ d^{-1}$ was determined ($n = 3$). From this dark respiration rate a k_D of $0.31 \pm 0.02\ d^{-1}$ was calculated (Appendix B). Subsequently, μ_{max} and θ could be determined using the obtained value for k_D, μ_{ref} of the two light limited steady states, and the highest reported net specific growth rate for *N. oleobundans* with sufficient information on the average light supply rate ($1.92\ d^{-1}$ at an average light supply rate of 300 $\mu mol\ m^{-2}\ s^{-1}$ (Santos et al., 2012)). This resulted in values of $2.17\ d^{-1}$ for μ_{max} and 0.28 m^2 mol^{-1} for θ (Fig. 4A, $R^2 = 0.99$), and sets the maximum possible net specific growth rate in the model to $\mu_{max} - k_D = 1.86 \pm 0.02\ d^{-1}$.

4.1.5.2. Nitrogen limitation: $F_N = r_N$. To calculate μ under nitrogen limitation, the nitrate balance and the nitrogen atom balance were combined, giving:

$$\mu = \frac{r_N}{f_{N.x} \cdot C_X} \quad (17)$$

In previous work, it was shown that $f_{N.x}\ C_X$ (assimilated nitrogen in functional biomass, $g\ m^{-3}$) is constant in a turbidostat, due to the relation between the turbidity in a system and the total amount of nitrogen assimilated (Childers and Gosselink, 1990; Klok et al., 2013). In Fig. 4B, the measured μ is plotted against r_N. Linear regression with intercept zero gave $f_{N.x}\ C_X = 57 \pm 1.6\ g\ m^{-3}$ ($R^2 = 0.98$), which is comparable to the average measured value ($58 \pm 4.2\ g\ m^{-3}$; Appendix A). As Eqs. (17) is valid under both nitrogen replete as well as nitrogen limited conditions, combination with Eq. (15) gives the value of $r_{N.ref}$, the nitrogen consumption rate achieved under light limitation under a given light regime, which is used in Eq. (13) and (14).

It should be noted that modelling cultures which are more dilute than those described here, requires experimental evaluation of $f_N\ C_X$, or an additional equation that describes the relation between achieved turbidity and nitrogen assimilated in functional biomass. In absence of such data, the model is limited to describing cultures with approximately 90% light absorption.

4.1.6. Absorptive cross section

The change of the absorptive cross section (α_X) in response to changes in environmental conditions is known as photoacclimation. Geider et al. developed several models that describe photoacclimation as a function of light and nutrient availability, and correlated photoacclimation to the ratio of actually achieved and maximum potential photosynthesis rates (Geider et al., 1997). This ratio quantifies the balance between energy demand and supply in the chloroplast, and can be seen as a measure of the reduction state of the plastoquinone pool, which is the primary signal responsible for regulation of light harvesting complex proteins (Escoubas et al., 1995).

A similar 'photosynthetic ratio' was calculated from the experimental data by dividing the number of electrons used to form biomass constituents X, T and S, by the number of electrons that could potentially be generated from the absorbed light ($r_{Ph}/Y_{Ph.e}$). Evaluating α_X, expressed as $m^2\ g^{-1}$ of functional biomass, as a function of this ratio revealed a linear relationship:

$$\alpha_X = \sigma_\alpha \cdot \left(\frac{r_X/Y_{X.e} + r_S/Y_{S.e} + r_T/Y_{T.e}}{r_{Ph}/Y_{Ph.e}} \right) + \alpha_{X.min} \quad (18)$$

Fitting this equation to the experimental data resulted in values of $0.235 \pm 0.032\ m^2\ g^{-1}$ and $0.023 \pm 0.009\ m^2\ g^{-1}$ for σ_a and $\alpha_{X.min}$, respectively ($R^2 = 0.88$, Fig. 4C). $\alpha_{X.min}$ can be regarded as the hypothetical minimum absorptive cross section of functional biomass for capturing light energy under severe nitrogen shortage or extremely high light intensities at steady state growing conditions.

4.1.7. Scattering

Lambert–Beer's law, which was adopted in this model, does not account for scattering of light by cells and thus effectively overestimates the light falling through a suspension. Several more accurate models exist in literature that do take scattering into account (Yun and Park, 2001), but due to the complexity of these models, a more simple solution was adopted by multiplying the light path with a scattering coefficient S (−) (Eq. (3)). The relation between the measured scattering coefficient S (−) and the total biomass concentration ($C_{TOTAL} = C_X + C_S + C_T$) in the system was derived

Table 2
Auxiliary model equations (A) and summary of measured and calculated parameters (B). Standard deviations (indicated with ±) are based on $n = 3$ (for k_D), $n = 8$ (for σ_S and σ_M) and $n = 9$ (other parameters).

A

#	Equation
[10]	$\frac{r_X}{Y_{X.e}} = \sigma_N \cdot r_N$
[11]	$\frac{r_S}{Y_{S.e}} = \sigma_S \cdot \sigma_N \cdot r_N + \sigma_M \cdot \frac{r_{Ph}}{Y_{Ph.e}}$
[13]	$\frac{r_T}{Y_{T.e}} = \sigma_T \cdot \sigma_N \cdot (1 + \sigma_S) \cdot (r_{N.ref} - r_N)$
[15]-[17]	$\mu = \min[\mu_{max} \cdot \tanh\left(\frac{\theta \cdot J_{Ph.av} \cdot 3600 \cdot 24 \cdot 10^{-6}}{\mu_{max}}\right) - k_D, \mu = \frac{r_N}{f_N \cdot C_X}]$
[18]	$\alpha_X = \sigma_\alpha \cdot \left(\frac{r_X/Y_{X.e} + r_S/Y_{S.e} + r_T/Y_{T.e}}{r_{Ph}/Y_{Ph.e}}\right) + \alpha_{X.min}$
[19]	$S = (C_X + C_S + C_T) \cdot \sigma_{Scat} + 1$

B

Parameter	Value	Units	Parameter	Value	Units
σ_N	2.38 ± 0.04	mol e^- (g N)$^{-1}$	μ_{max}	2.17	d^{-1}
σ_S	0.112	mol m^{-3}	θ	0.28	$m^2\ mol^{-1}$
σ_M	0.038	mol m^{-3}	k_D	0.31 ± 0.02	d^{-1}
σ_T	0.086 ± 0.005	mol mol^{-1}	$f_N \cdot C_X$	57 ± 1.6	$g\ m^{-3}$
$Y_{T.E}$	2.78	g mol^{-1}	σ_a	0.235 ± 0.032	$m^2\ g^{-1}$
$Y_{S.E}$	6.76	g mol^{-1}	$\alpha_{X.min}$	0.023 ± 0.009	$m^2\ g^{-1}$
$Y_{Ph.e}$	2	mol γ (mol e^-)$^{-1}$	σ_{Scat}	$6.6 \times 10^{-4} \pm 1.9 \times 10^{-4}$	$m^3\ g^{-1}$
δ_{pbr}	0.02	m			

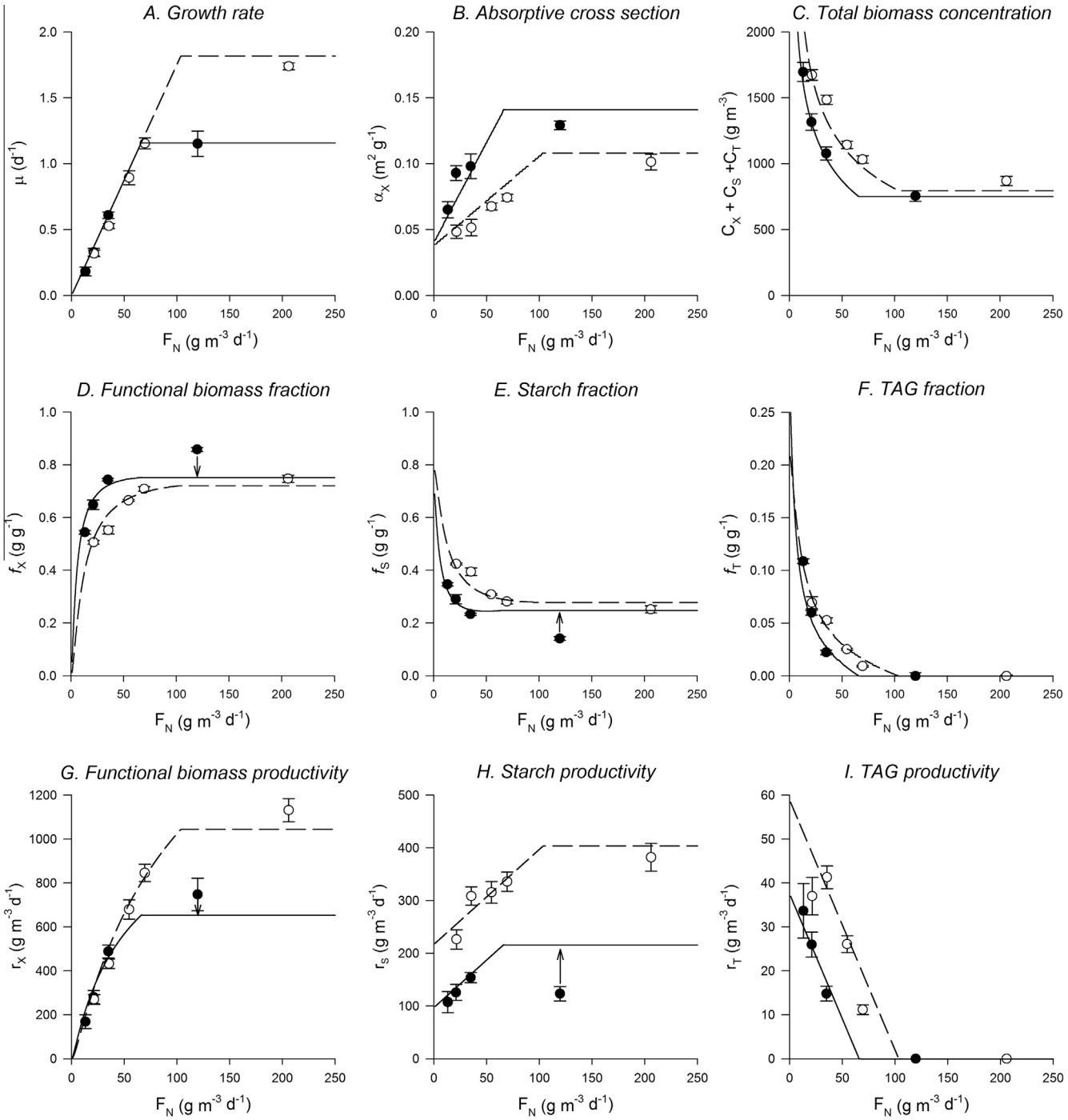

Fig. 5. Model simulations of specific growth rate (A); absorptive cross section (B); total biomass concentration (C); mass fractions of functional biomass (D), starch (E) and TAG (F); volumetric productivities of functional biomass (G), starch (H) and TAG (I). Closed circles represent experiments that were performed under low light conditions, open circles represent experiments performed under high light conditions. The arrows indicate the respective under- and overestimation of functional biomass and starch under light limited conditions (see Section 4.1.2).

from the experimental data using Eq. (3). By setting $S \geqslant 1$, a linear relation was found (Fig. 4D):

$$S = (C_X + C_S + C_T) \cdot \sigma_{Scat} + 1 \quad (19)$$

with $\sigma_{Scat} = 6.6 \times 10^{-4} \pm 1.9 \times 10^{-4}$ ($m^3\ g^{-1}$) and $R^2 = 0.73$.

A summary of all auxiliary equations and their parameters discussed in this section can be found in Table 2.

4.2. Model predictions

Fig. 5 shows the model predictions and the measured data for the two tested light intensities at several nitrogen supply rates. Within the experimental range, the model describes the measured variables very well.

The model can be used to predict biomass composition (i.e. the fractions of X, S and T), production rates and yields of the biomass components in a nitrogen limited turbidostat outside the

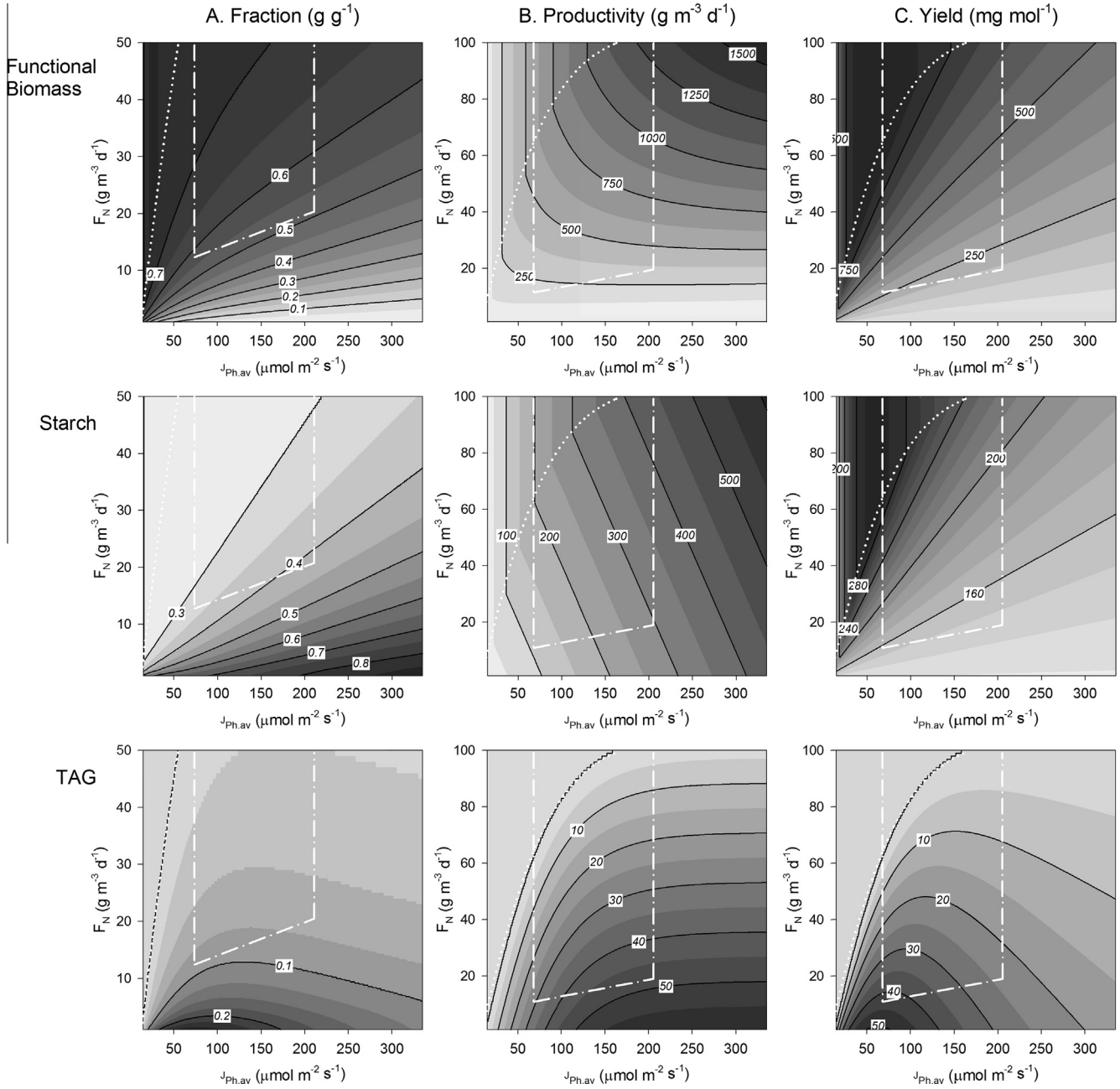

Fig. 6. Model predictions of functional biomass high in proteins (upper graphs), starch (middle graphs) and TAG (lower graphs) fractions (A), productivity (B) and yield on light (C) for combinations of nitrogen and average light supply rates, at 90% light absorption over the system. The experimental range is indicated by white dashed lines. The white dotted line represents the transition between light and nitrogen limitation. This line follows from the hyperbolic tangent model for the light-limited specific growth rate and this line coincides with the minimal F_N necessary for TAG accumulation.

experimental range, provided that 90% of the light is absorbed in the system (Fig. 6). These predictions can be used to find the optimal cultivation conditions for functional biomass, starch and TAG.

To evaluate the optimal cultivation conditions for each biomass component, three parameters were considered. First of all, the mass fraction of the component of interest (Fig. 6A), as this is an important parameter for product recovery. Secondly, the volumetric production rate (Fig. 6B), as this reflects the photobioreactor performance. Finally the yield of the product on light (Fig. 6C) was calculated, which is an indicator of how efficiently light energy is used for biosynthesis of that product. This yield is a parameter that facilitates direct comparison of algae strains and photobioreactor performance of different reactor types and operation strategies. Moreover, yield on light is directly proportional to the aerial productivity, an important parameter to consider when optimising commercial outdoor production of any microalgal product, since in outdoor production the amount of light available per surface area is limiting.

4.2.1. Functional biomass and protein

Functional biomass is rich in proteins, and the model predictions for functional biomass can therefore directly be translated into recommendations for protein production. Nitrogen limitation is not beneficial for both functional biomass and protein content, productivity and yield, since nitrogen is vital for protein synthesis. This is reflected by the model predictions, where functional

biomass content, productivity and yield are lower under nitrogen limited conditions. As can be seen in the upper row of Fig. 6, increasing average light intensities will increase the functional biomass volumetric production rate. It will reach its maximum value under nitrogen repletion and at the average light supply rate at which μ_{max} is reached in the system. However, increasing the average light intensity will be at the expense of content and yield. The yield is optimal under low average light supply rates, as light is used most efficiently under these conditions (Goldman, 1979). The content is highest under these conditions because starch production rates are low and TAG is not produced at all. Therefore, nitrogen replete conditions combined with a low average light supply rate is the preferred window of operation for functional biomass, and thus protein production.

4.2.2. Starch

As starch synthesis is coupled to the production of functional biomass (see Section 4.1.2), starch productivity will be lower when growth is hampered by nitrogen limitation. The highest starch production rates are thus found under light limited conditions, with high average light intensities. However, nitrogen limitation must be applied when aiming at starch contents above 30%, as this will lower the functional biomass productivity. It should be noted that under light limited conditions at low light supply rates, the model overestimates starch production rates (see Section 4.1.2) and starch yields. However, it is not expected that this overestimation affects the trend predicted by the model, i.e.: starch yield on light is optimal under low average light supply rates and nitrogen replete conditions. In short, the optimal conditions for starch content (high light, low N), volumetric productivity (high light, sufficient N) and yield (low light, sufficient N) are found under very different cultivation conditions.

4.2.3. TAG

Storage lipid productivity is highest at minimal nitrogen supply rate, and the optimum is found under high light supply rates because under these conditions the maximum electron excess is created. The model simulations show that high volumetric TAG production rates and high TAG contents are mutually exclusive, because the necessary increased light supply will result in more starch to be produced as well. The highest TAG contents are thus found under lower average light supply rates (roughly between a J_{av} of 50 and 150 μmol m^{-2} s^{-1}), where the starch production rate is less high. Interestingly, the optimum for TAG yield on light seems to coincide with the optimum for TAG content (between a J_{av} of 50 and 100 μmol m^{-2} s^{-1}), which makes lower light supply rates and severe nitrogen limitation favourable cultivation conditions for TAG production in a nitrogen limited turbidostat. The optima for TAG production predicted by the model are in agreement with findings in batch experiments with *Scenedesmus obliquus*, where nitrogen run-outs led to higher TAG yields under low light supply rates (Breuer et al., 2013).

4.3. Model limitations and implications

When extrapolating, it must be kept in mind that the model predictions are less certain if the system approaches complete nitrogen depletion (F_N = 0 g m d^{-1}). It is questionable whether it is even possible to run a system continuously in steady state with extremely low nitrogen supply rates, since the functional biomass production rate, and thus also the mass fraction of viable cell material, approaches zero. Also, it is possible that some of the calculated starch fractions (f_S > 0.8 g g^{-1}) cause a physical limitation for cell functioning and division under these conditions. In the model definition for r_L, energy use for cellular maintenance is not distinguished from energy losses in dissipation processes and also not from energy use for the synthesis and assembly of biomass constituents (growth associated maintenance). Therefore, the results predicted for very low light intensities will diverge, as under these conditions, cellular maintenance will become a larger energy sink than growth associated maintenance (Kliphuis et al., 2012). The increasing importance of maintenance at very low average light intensities could, for example, become important when optimising functional biomass content and yield, and starch yield on light, as their optima are found under these conditions. Similarly, the model predictions can deviate for extremely high light intensities since damaging processes such as photoinhibition, which is not taken into account in the model, can cause an increase in maintenance requirement. Nevertheless, as this model has a physiological basis, it can be used to calculate the trends in biomass composition, and in production rates and yields of the separate components as a function of nitrogen and light supply, and the model outcomes can be used as an indication for the optimal cultivation conditions for tailor-made biomass in a nitrogen limited turbidostat.

As the work presented here describes a continuous process, the question rises whether it can be directly applied to discontinuous processes, such as the commonly used batch nitrogen starvation approach used for the production of TAG-rich biomass. It is expected that translation of the model equations is only partly possible as the process described here is in a steady state, which means that the algae are fully adapted to environmental conditions, while during nitrogen starvation, these conditions are constantly changing. This means that the 'rates of change' as a function of environmental conditions should be known, where applicable. For example, modelling starch synthesis will require some additional regulatory terms, that allow for describing the down regulation of starch synthesis after growth is halted. Furthermore, it should be further investigated whether the fixed percentage of excess electrons ending up in TAG is also observed under nitrogen starvation conditions, or in other algal species.

On the other hand, it is expected that the biological principles, such as TAG synthesis being a result of an electron excess, decreased light use efficiency under high light and/or limiting nitrogen supply rates, and electrons ending up functional biomass being proportional to the available nitrogen are not dependent on the process used. Moreover, as the locations of several predicted optima coincide with results obtained for batch cultivation, it is expected that the trends predicted by the presented model can indeed be generalised.

From the model predictions it can be concluded that each biomass component requires very distinct cultivation conditions, and that optimising for a certain compound is always a compromise between yield, content and/or volumetric productivity. Also, a profitable production process will rely on many more factors than those calculated by the model (i.e. productivity, content and yield), such as development of inexpensive harvesting methods, low-cost photobioreactors and additional biorefinery, in order to maximise the potential profit that can be made on biomass components. However, the biological model presented here is a good starting point for further development and modelling of continuous production chains for commercial microalgal products.

5. Conclusion

A kinetic model was presented based on the electron distribution in *N. oleoabundans*, grown at several light and nitrogen supply rates. It was shown that starch acts as growth-related storage component, whereas TAG is only overproduced if an excess of electrons is generated due to nitrogen limitation. The proposed model describes the experimental data well and shows that by manipulating the cultivation conditions in a nitrogen limited turbidostat, algal

biomass composition, and the volumetric productivities and yields on light of each of the major biomass constituents (protein, starch and TAG) can be controlled on demand.

Acknowledgements

This work was performed in the TTIW-cooperation framework of Wetsus, Centre of Excellence for Sustainable Water Technology (http://www.wetsus.nl). Wetsus is funded by the Dutch Ministry of Economic Affairs. The authors like to thank the members of the theme 'Algae' from Wetsus for the discussions and their financial support.

Appendix A. Supplementary data

Supplementary data associated with this article can be found, in the online version, at http://dx.doi.org/10.1016/j.biortech.2013.07.039.

References

Ball, S.G., Dirick, L., Decq, A., Martiat, J.-C., Matagne, R., 1990. Physiology of starch storage in the monocellular alga *Chlamydomonas reinhardtii*. Plant Sci. 66, 1–9.

Breuer, G., Lamers, P.P., Martens, D.E., Draaisma, R.B., Wijffels, R.H., 2013. Effect of light intensity, pH, and temperature on triacylglycerol (TAG) accumulation induced by nitrogen starvation in *Scenedesmus obliquus*. Bioresour. Technol. 143, 1–9.

Childers, D.L., Gosselink, J.G., 1990. Assessment of cumulative impacts to water quality in a forested wetland landscape. J. Environ. Qual. 19, 455–464.

Cohen, D., Parnas, H., 1976. An optimal policy for the metabolism of storage materials in unicellular algae. J. Theor. Biol. 56, 1–18.

Escoubas, J.M., Lomas, M., LaRoche, J., Falkowski, P.G., 1995. Light intensity regulation of cab gene transcription is signaled by the redox state of the plastoquinone pool. PNAS 92, 10237–10241.

Geider, R.J., Macintyre, H.L., Kana, T.M., 1997. Dynamic model of phytoplankton growth and acclimation: responses of the balanced growth rate and the chlorophyll a: carbon ratio to light, nutrient-limitation and temperature. Mar. Ecol. Prog. Ser. 148, 187–200.

Goldman, J.C., 1979. Outdoor algal mass cultures – II. Photosynthetic yield limitations. Water Res. 13, 119–136.

Harrison, P.J., Thompson, P.A., Calderwood, G.S., 1990. Effects of nutrient and light limitation on the biochemical composition of phytoplankton. J. Appl. Phycol. 2, 45–56.

Harrison, S.T.L., Richardson, C., Griffiths, M.J., 2013. Analysis of microalgal biorefineries for bioenergy from an environmental and economic perspective focus on algal biodiesel. In: Bux, F. (Ed.), Biotechnological Applications of Microalgae: Biodiesel and Value Added Products. CRC Press, Boca Raton, pp. 113–136.

Hu, Q., Sommerfeld, M., Jarvis, E., Ghirardi, M., Posewitz, M., Seibert, M., Darzins, A., 2008. Microalgal triacylglycerols as feedstocks for biofuel production: perspectives and advances. Plant J. 54, 621–639.

Huppe, H.C., Turpin, D.H., 1994. Integration of carbon and nitrogen metabolism in plant and algal cells. Annu. Rev. Plant Physiol. Plant Mol. Biol. 45, 577–607.

Kliphuis, A.M.J., Klok, A.J., Martens, D.E., Lamers, P.P., Janssen, M., Wijffels, R.H., 2012. Metabolic modeling of *Chlamydomonas reinhardtii* energy requirements for photoautotrophic growth and maintenance. J. Appl. Phycol. 24, 253–266.

Klok, A.J., Martens, D.E., Wijffels, R.H., Lamers, P.P., 2013. Simultaneous growth and neutral lipid accumulation in microalgae. Bioresour. Technol. 134, 233–243.

Kolber, Z., Zehr, J., Falkowski, P., 1988. Effects of growth irradiance and nitrogen limitation on photosynthetic energy conversion in photosystem II. Plant Physiol. 88, 923–929.

Ledford, H.K., Niyogi, K.K., 2005. Singlet oxygen and photo-oxidative stress management in plants and algae. Plant Cell Environ. 28, 1037–1045.

Li, Y., Han, D., Hu, G., Sommerfeld, M., Hu, Q., 2010. Inhibition of starch synthesis results in overproduction of lipids in *Chlamydomonas reinhardtii*. Biotechnol. Bioeng. 107, 258–268.

Li, Y., Han, D., Sommerfeld, M., Hu, Q., 2011. Photosynthetic carbon partitioning and lipid production in the oleaginous microalga *Pseudochlorococcum* sp. (*Chlorophyceae*) under nitrogen-limited conditions. Bioresour. Technol. 102, 123–129.

Li, Y., Han, D., Yoon, K., Zhu, S., Sommerfeld, M., Hu, Q., 2013. Molecular and cellular mechanisms for lipid synthesis and accumulation in microalgae: biotechnological implications. In: Richmond, A., Hu, Q. (Eds.), Handbook of Microalgal Culture: Biotechnology and Applied Phycology, second ed. Wiley-Blackwell, Chichester, pp. 545–565.

Liu, B., Benning, C., 2013. Lipid metabolism in microalgae distinguishes itself. Curr. Opin. Biotechnol. 24, 300–309.

Mairet, F., Bernard, O., Masci, P., Lacour, T., Sciandra, A., 2011. Modelling neutral lipid production by the microalga *Isochrysis aff. galbana* under nitrogen limitation. Bioresour. Technol. 102, 142–149.

Mata, T.M., Martins, A.A., Caetano, N.S., 2010. Microalgae for biodiesel production and other applications: a review. Renewable Sustainable Energy Rev. 14, 217–232.

Meeuwse, P., Tramper, J., Rinzema, A., 2011. Modeling lipid accumulation in oleaginous fungi in chemostat cultures: I. Development and validation of a chemostat model for *Umbelopsis isabellina*. Bioprocess Biosyst. Eng. 34, 939–949.

Melis, A., 1999. Photosystem-II damage and repair cycle in chloroplasts: what modulates the rate of photodamage in vivo? Trends Plant Sci. 4, 130–135.

Packer, A., Li, Y., Andersen, T., Hu, Q., Kuang, Y., Sommerfeld, M., 2011. Growth and neutral lipid synthesis in green microalgae: a mathematical model. Bioresour. Technol. 102, 111–117.

Pan, Y.-Y., Wang, S.-T., Chuang, L.-T., Chang, Y.-W., Chen, C.-N.N., 2011. Isolation of thermo-tolerant and high lipid content green microalgae: oil accumulation is predominantly controlled by photosystem efficiency during stress treatments in *Desmodesmus*. Bioresour. Technol. 102, 10510–10517.

Platt, T., Jassby, A.D., 1976. The relationship between photosynthesis and light for natural assemblages of coastal marine phytoplankton. J. Phycol. 12, 421–430.

Quinn, J., de Winter, L., Bradley, T., 2011. Microalgae bulk growth model with application to industrial scale systems. Bioresour. Technol. 102, 5083–5092.

Richmond, A., 2004. Principles for attaining maximal microalgal productivity in photobioreactors: an overview. In: Ang, P.O., Jr. (Ed.), Asian Pacific Phycology in the 21st Century: Prospects and Challenges. Springer, Dordrecht, Netherlands, pp. 33–37.

Rismani-Yazdi, H., Haznedaroglu, B., Hsin, C., Peccia, J., 2012. Transcriptomic analysis of the oleaginous microalga *Neochloris oleoabundans* reveals metabolic insights into triacylglyceride accumulation. Biotechnol. Biofuels 5, 1–16.

Santos, A.M., Janssen, M., Lamers, P.P., Evers, W.A.C., Wijffels, R.H., 2012. Growth of oil accumulating microalga *Neochloris oleoabundans* under alkaline-saline conditions. Bioresour. Technol. 104, 593–599.

Sousa, C., de Winter, L., Janssen, M., Vermuë, M.H., Wijffels, R.H., 2012. Growth of the microalgae *Neochloris oleoabundans* at high partial oxygen pressures and sub-saturating light intensity. Bioresour. Technol. 104, 565–570.

Turpin, D.H., 1991. Effects of inorganic N availability on algal photosynthesis and carbon metabolism. J. Phycol. 27, 14–20.

Wijffels, R.H., Barbosa, M.J., Eppink, M.H.M., 2010. Microalgae for the production of bulk chemicals and biofuels. Biofuels, Bioprod. Bioref. 4, 287–295.

Yun, Y.S., Park, J.M., 2001. Attenuation of monochromatic and polychromatic lights in *Chlorella vulgaris* suspensions. Appl. Microbiol. Biotechnol. 55, 765–770.